Adaptive Pruning Method of Digital PreDistortion Models Based on DLA Algorithm for LTE/5G Applications

Zixiao YANG[1], Smail BACHIR[1], Claude DUVANAUD[1], Jean-Marc OUVRARD[2] and Thomas GAMBIER[2]

***Abstract*— This paper proposes an adaptive pruning method for digital predistortion using a direct learning architecture. To linearize RF power amplifiers, the Generalized Memory Polynomial model is widely used as an inverse dynamical function. However, due to its large number of required terms, many studies focus on reducing implementation complexity. This work mainly uses the doubly orthogonal matching pursuit approach to select active terms while incorporating the Levenberg-Marquardt algorithm to enhance linearization performance. The proposed method achieves a linearity performance nearly equivalent to that of the full model, while significantly reducing the search time for the optimal structure. It's applied to the linearization of an Open Radio Station for LTE/5G applications, including an asymmetrical two-stage 10W Doherty power amplifier implemented in GaN technology. Comparisons with other state-of-the-art approaches, such as the Gradient method and the Least-Squares algorithm, demonstrate that the proposed method achieves better linearization performance in terms of spectral regrowths reduction and lower computational complexity.**

I. Introduction

With the rapid evolution of modern wireless communication systems and the emergence of new generations of radiocommunication focused on high data rates and spectral efficiency, Power Amplifiers (PAs) remain one of the critical components in RF front-end design. Indeed, operating PAs in the high-efficiency region (near saturation) introduces strong nonlinearities, which degrade signal quality and system performance. To mitigate the nonlinearities and memory effects [1] [2] [3] and enhance linearity performance, Digital Pre-Distortion (DPD), which inserts a linearizer upstream of the baseband system, has been proposed as an effective solution [4] [5].

In real-time linearization, several approaches have been proposed in the literature with two main techniques: direct learning architecture (DLA) [6] and indirect learning architecture (ILA) [1], [7]. In the ILA, a postdistorter is determined iteratively to update the complex coefficients of the predistorter, while the DLA consists on identifying the PA nonlinear model to estimate the predistorter by minimizing a criterion based on the difference between the measured PA output and the transmitted input. Under noisy measurements, studies in [8] [9] demonstrate a higher level of robustness and accuracy for the DLA compared to the ILA.

[1]Zixiao YANG, Smail BACHIR and Claude Duvanaud are with XLIM Laboratory, UMR CNRS 7252, University of Poitiers, France.

[2]Jean-Marc OUVRARD and Thomas GAMBIER are with RapidSpace International, Paris, France.

Corresponding author: zixiao.yang@univ-poitiers.fr

The effectiveness of the DPD depends not only on the architecture, but also on the accuracy of the predistorter model. Various DPD models, such as the Volterra Series [10] and its variations (Hammerstein and Wiener models) [5], Memory Polynomial (MP) [11], Generalized Memory Polynomial (GMP) [12], cascaded models [13], and segmentation-based models [14], have been widely used [5]. Among these, the GMP model is mainly used due to its effectiveness in capturing PA memory effects and nonlinearities [15]. Its practical implementation can be seen in the latest Analog Devices AD9375 chip, which integrates a DPD engine based on the GMP model, supporting signal bandwidths up to 40 MHz. However, the high number of coefficients in GMP significantly increases computational complexity as the number of required terms increase [16].

Several studies have been carried out to eliminate iteratively the non-efficient coefficients in the GMP model, according to their contribution in the Normalized Mean Square Error (NMSE) and/or in the Adjacent Channel Power Ratio (ACPR) descent [2]. This work deals with this topic and aims to propose a recursive method for pruning insignificant GMP terms combined with the DLA to estimate the inverse PA's model with low complexity. The proposed algorithm combines the Doubly Orthogonal Matching Pursuit (DOMP) method [17] to prune the GMP model and the Levenberg-Marquardt algorithm (L-M) [18] [19] for real-time parameter estimation. The DOMP mainly based on correlation between regressor vectors and the output residual to select the active terms. L-M algorithm is a trade-off between the robustness of the Gradient descent and the speed of Gauss-Newton method [18]. This approach has been tested to linearize a Doherty GaN hybrid 10W PA designed for the LTE/5G signals with a bandwidth of 20 MHz and a transmission frequency of 3.65 GHz. For evaluation, the DPD model and algorithm have been implemented using a Software-Defined Radio platform with a sampling rate of 61.44 MHz.

The remainder of this contribution is organized as follows. First, Section II covers the theoretical part and introduces the adaptive pruning DLA method, which mainly discusses the DOMP method and the L-M algorithm. The DPD experimental results are detailed in Section III. Finally, Section IV summarizes the main results and concludes this paper.

II. Adaptive Pruning Direct Learning Architecture Method

Fig. 1 describes the general principle of the proposed method based on the DLA with the L-M algorithm.

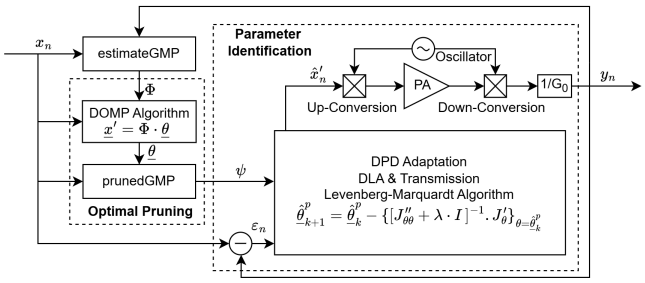

Fig. 1: Adaptive DPD based on DLA with L-M algorithm

Using a feedback path that measures the normalized output y_n (where G_0 is the PA's linear gain), this real-time technique is based on two main blocks:

- a first called "Optimal Pruning" that prunes the set of inactive terms in the GMP model,
- and the "Parameter Identification" block, which improves the estimation of the pruned structure.

In the following, we will detail the common set of instructions between Fig. 1 and the corresponding algorithm presented in Table I.

A. The GMP model

The relationship between the DPD output x'_n and the transmitted signal x_n in baseband can be expressed according to the GMP system given by the following expression [1] :

$$\begin{aligned} x'_n &= \underline{\varphi}_n^T \cdot \underline{\theta} \\ &= \sum_{k=0}^{K_a-1} \sum_{l=0}^{L_a-1} a_{kl} \cdot x_{n-l} \cdot |x_{n-l}|^k \\ &\quad + \sum_{k=1}^{K_b} \sum_{l=0}^{L_b-1} \sum_{m=1}^{M_b} b_{klm} \cdot x_{n-l} \cdot |x_{n-l-m}|^k \\ &\quad + \sum_{k=1}^{K_c} \sum_{l=0}^{L_c-1} \sum_{m=1}^{M_c} c_{klm} \cdot x_{n-l} \cdot |x_{n-l+m}|^k \end{aligned} \tag{1}$$

where

$(\cdot)^T$ and $|\cdot|$ are, respectively, transpose function and the absolute value,

K_a, K_b and K_c represent the nonlinear order of the power series,

L_a, L_b and L_c are the memory depths,

M_b and M_c respectively, the lagging and leading cross-terms.

$\underline{\varphi}_n^{N_c \times 1}$ is the vector of regressor and $\underline{\theta}^{N_c \times 1}$ is the vector of parameters to be estimated, such as:

$$\underline{\varphi}_n = \begin{bmatrix} x_n \\ \vdots \\ x_{n-L_a+1} \cdot |x_{n-L_a+1}|^{K_a-1} \\ x_n \cdot |x_{n-1}| \\ \vdots \\ x_{n-L_b+1} \cdot |x_{n-L_b+1-M_b}|^{K_b} \\ x_n \cdot |x_{n+1}| \\ \vdots \\ x_{n-L_c+1} \cdot |x_{n-L_c+1+M_c}|^{K_c} \end{bmatrix}, \underline{\theta} = \begin{bmatrix} a_{00} \\ \vdots \\ a_{(K_a-1)(L_a-1)} \\ b_{101} \\ \vdots \\ b_{K_b(L_b-1)M_b} \\ c_{101} \\ \vdots \\ c_{K_c(L_c-1)M_c} \end{bmatrix}$$

$N_c = K_a \cdot L_a + K_b \cdot L_b \cdot M_b + K_c \cdot L_c \cdot M_c$ is the number of coefficients.

For a measurement of N samples, we can write the following matrix expression:

$$\underline{x}' = \Phi \cdot \underline{\theta} \tag{2}$$

where $\Phi^{N \times N_c}$ is the full regression matrix:

$$\Phi = \begin{bmatrix} \underline{\varphi}_1^T \\ \underline{\varphi}_2^T \\ \vdots \\ \underline{\varphi}_N^T \end{bmatrix} \tag{3}$$

The main problem with the GMP model is its high computational complexity, overfitting and term redundancy. The model includes many polynomial and memory terms, leading to high-dimensional parameter estimation N_c, which can be inefficient and computationally expensive. Many terms contribute minimally to modeling accuracy and should be eliminated. In the next section, we propose a new technique to reduce the number of regressors in the full-matrix Φ to retain only the most contributive terms in describing the PA's inverse behavior.

B. Pruning method based on Direct Learning Architecture and Levenberg-Marquardt Algorithm

The proposed algorithm is illustrated in Table I. It's based on a performance evaluation loop using the obtained ACPR values and the maximum number of coefficients in the GMP model noted n_{max}, which corresponds in practice to the possibilities of implementation on the final target.

After setting the desired threshold value of the ACPR $\mathcal{M}$, the maximum number of coefficients n_{max}, the number of iterations n_{iter} required for the convergence of the L-M algorithm and the monitoring parameter λ, a first measurement of the complex envelope of input x and output y is performed. The output value of the ACPR without DPD is also computed using the FFT on the measured output [12].

Using y as input and x as output, we perform an initial estimation of the PA's inverse model by Least-Squares (LS). The aim is to generate the full-regression matrix Φ, which will be pruned using the DOMP algorithm and serves as

Adaptive Pruning DLA Algorithm

Set $\mathcal{M}$, n_{max}, n_{iter}, λ
Get $\underline{x}$, $\underline{y}$ and acpr # The 1st measurement
1: $\underline{\theta}, \Phi \leftarrow \mathbf{estimateGMP}(\underline{y}\ ,\ \underline{x})$ # PA inverse estimation
2: $\mathbf{Z}_0 = \Phi, \quad \underline{e}_0 \leftarrow \underline{x}, \quad \Psi_0 \leftarrow \{\}, \quad n_t = 1$
3: **while** ($n_t < n_{max}$ or acpr $> \mathcal{M}$) **do**

Loop for optimal pruning based on DOMP algorithm
4: **for** t = 0 to $n_t - 1$ **do**
5: $\mathbf{Z}_t^{\{i\}} \leftarrow \frac{\mathbf{z}_t^{\{i\}}}{\|\mathbf{z}_t^{\{i\}}\|_2}, \quad i \notin \mathbf{S}_t$ # $||\cdot||_2$: Euclidean norm
6: $i_{t+1} \leftarrow \arg\max_{i \notin \mathbf{S}_t} \left| \mathbf{Z}_t^{\{i\}} \cdot \underline{e}_t \right|$
7: $\mathbf{S}_{t+1} \leftarrow \mathbf{S}_t \cup i_{t+1}$
8: $\Psi_{t+1} \leftarrow \Phi\,[\mathbf{S}_{t+1}]$
9: $\mathbf{p}_t \leftarrow \left(\mathbf{Z}_t^{\{i_t\}}\right)^H \cdot \mathbf{Z}_t$
10: $\mathbf{Z}_{t+1} \leftarrow \mathbf{Z}_t - \mathbf{p}_t \otimes \mathbf{Z}_t^{\{i_t\}}$ # $\otimes$: Kronecker product
11: $\underline{\theta}_{t+1} \leftarrow \left(\Psi_{t+1}^H \cdot \Psi_{t+1}\right)^{-1} \cdot \Psi_{t+1}^H \cdot \underline{x}$
12: $\underline{x}'_{t+1} \leftarrow \Psi_{t+1} \cdot \underline{\theta}_{t+1}$
13: $\underline{e}_{t+1} \leftarrow \underline{x} - \underline{x}'_{t+1}$ # Update the residual
14: **end for**
15: $\hat{\underline{\theta}}_0^p \leftarrow \underline{\theta}_{n_t}$ # Working now with the new pruned basis
16: $\hat{\underline{x}}', \psi \leftarrow \mathbf{prunedGMP}(\underline{x}\ , \hat{\underline{\theta}}_0^p)$ # Pruned DPD simulation

Parameter identification based on Levenberg-Marquardt algorithm
17: **for** k = 0 **to** $n_{iter} - 1$ **do**
18: Transmit the new DPD signal $\hat{\underline{x}}'$
19: Get PA output $\underline{y}$ and I/O synchronization using cross-correlation
20: $\hat{\underline{\theta}}_{k+1}^p = \hat{\underline{\theta}}_k^p - \{[J''_{\theta\theta} + \lambda \cdot I\,]^{-1}.J'_\theta\}_{\theta = \hat{\underline{\theta}}_k^p}$
21: $\lambda \leftarrow \lambda/10$ # To speed-up the convergence
22: $\underline{\varepsilon} = \underline{x} - \underline{y}$
23: $\text{nmse}_{k+1} \leftarrow 10 \cdot \log_{10}\left[\frac{\underline{\varepsilon}^H \cdot \underline{\varepsilon}}{\underline{x}^H \cdot \underline{x}}\right]$ # Normalized Mean-Square Error
24: $\hat{\underline{x}}' \leftarrow \psi \cdot \hat{\underline{\theta}}_{k+1}^p$ # DPD output for the next iteration
25: **end for**
26: Update acpr
27: $n_t \leftarrow n_t + 1$
28: **end while**

TABLE I: Adaptive Pruning DLA Algorithm

an initialization of its orthogonal equivalent matrix $\mathbf{Z}_0$ in instruction 2. In addition, the residual vector $\underline{\varepsilon}_0$ is set to the value of the complex input envelope $\underline{x}$, and the pruned regression matrix Ψ_0 is initially empty. This matrix will gradually be filled with the regression vectors that form the new orthogonal basis. In this algorithm, $\mathbf{S}$ denotes the vector of indices locating the efficient regressors in the full-matrix Φ.

Model pruning can be performed by removing terms based on structured sparsity. In [17], the correlation between the regressors and the residuals was calculated to determine its relative importance, and terms with lower values were eliminated. In the t^{th} iteration, the highest normalized scalar resolution between the orthogonal matrix $\mathbf{Z}$, resulting on the ℓ_2 normalization of the regressors, and the residual $\underline{\varepsilon}$ is selected:

$$i_{t+1} \leftarrow \arg\max_{i \notin \mathbf{S}_t} \left| \mathbf{Z}_t^{\{i\}} \cdot \underline{\varepsilon}_t \right| \tag{4}$$

and the support $\mathbf{S}$ is increased by the selected component to form the new pruned matrix ψ (instructions 6–8).

The Gram-Schmidt orthogonalization is performed to obtain an orthogonal set of regression matrix $\mathbf{Z}$. The parameters are obtained using the LS algorithm and the vector of residual $\underline{e}$ is updated for the next iteration (instructions 11–13). Notice that matrix inversion in instruction 11 is performed using the Singular Value Decomposition (SVD) to reduce the computational complexity.

After selecting the orthogonal basis which includes the most significant terms of the DPD model, a second sub-loop is used to improve the parameter estimation (instructions 17–25). Indeed, the LS estimation from the first loop is highly sensitive to measurement noise and is often biased due to the correlation between the noise and the output. The application of Output Error algorithms (OE), such as the L-M algorithm, enables better convergence toward the optimum despite the presence of output noise [20]. The pruned vector of parameters $\hat{\underline{\theta}}^p$ is updated at each iteration such as:

$$\hat{\underline{\theta}}_{k+1}^p = \hat{\underline{\theta}}_k^p - \{[J''_{\theta\theta} + \lambda \cdot I\,]^{-1}.J'_\theta\}_{\theta = \hat{\underline{\theta}}_k^p} \tag{5}$$

where J is the quadratic criterion based on the estimation error expressed as:

$$J = \frac{1}{2}\sum_{n=1}^{N} \varepsilon_n^2 = \frac{1}{2}\,\underline{\varepsilon}^H\,\underline{\varepsilon} \tag{6}$$

with $\underline{\varepsilon} = \underline{x} - \underline{y}$ is the vector of error between the transmitted input and the measured output at each iteration. λ is the monitoring factor which controls the transition between the Gradient (high λ) and the Gauss-Newton (small λ). Thus, λ is divided by a factor of 10 to reach the speed convergence of the Gauss-Newton algorithm. J'_θ and $J''_{\theta\theta}$ are respectively the gradient and the hessian such as:

$$J'_\theta = -\sum_{n=1}^{N} \underline{\varepsilon}_n^H \cdot \underline{\sigma}_{y_{n,\underline{\theta}}} = -\psi^H \cdot \underline{\varepsilon} \tag{7}$$

and

$$J''_{\theta\theta} \approx \sum_{n=1}^{N} \underline{\sigma}_{y_{n,\underline{\theta}}} \cdot \underline{\sigma}_{y_{n,\underline{\theta}}}^H = \psi^H \cdot \psi \tag{8}$$

with $\sigma_{y_{n,\underline{\theta}}} = \frac{dy}{d\underline{\theta}}$ are the sensitivity function. I is the identity matrix and $(\cdot)^H$ is the transposition–conjugate transform.
In general, sensitivity functions are obtained, for each parameter, by partial differentiation of the studied system. When the model is linear in parameters, as in the case of the GMP model, the sensitivity functions are equal to the regressor ψ.

III. Experimental results

The experimental setup used to validate the proposed method is shown in Fig. 2. It consists of a 2-way/10 W Doherty PA module using GaN technology. The device under test (DUT) is designed for applications in 5G Massive MIMO systems, operating from 3.4 to 3.7 GHz. The selected Doherty amplifier can achieve a peak output power of 112 W in saturated mode and provides a linear gain of 30 dB. The PA is driven by an LTE/5G signal in FDD Duplex-Mode with 20 MHz bandwidth, 12 dB peak-to-average power

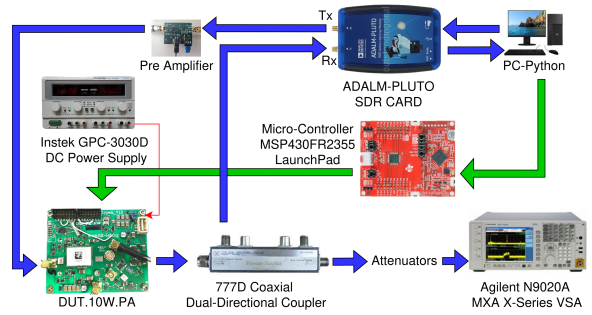

(a)

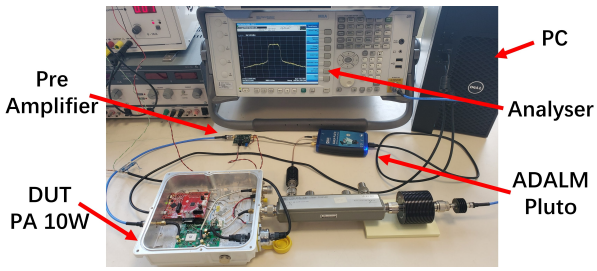

(b)

Fig. 2: Experimental benchmark. (a) Block-diagram. (b) Photograph of the experimental setup

ratio (PAPR) and 2^{16} samples at the carrier frequency of 3.65 GHz. The operating point is selected at an average power of 40 dBm, which corresponds to saturation mode. Fig. 2a is the experimental block-diagram and Fig. 2b is the real experimental setup. The proposed algorithm is implemented in Python language and the Adalm-Pluto board manages transmitted and received signals in real-time with a sampling rate of 61.44 MHz. At the receiver, a series of couplers and attenuators are inserted to visualize the spectrum on the Agilent N9020A MXA X-Series vector signal analyzer (VSA) and to obtain baseband signals via the RX-channel of the Adalm-Pluto. All these operations are made in real-time with computation of the ACPR and the Error Vector Magnitude (EVM) in the PC control.

For comparison, the proposed method, along with several others using DLA and ILA, was tested. For all methods, we used the same GMP model whose parameters are set as K_a = 6, L_a = 4, K_b = 4, L_b = 3, M_b = 3,K_c = 4,L_c = 3, M_c = 3. The above set of parameters can achieve optimal performance for the predistorter adapted to the chosen PA equipment. The algorithm's parameters have been chosen as $n_{max} = 40$ coefficients, $n_{iter} = 15$ iterations and $\lambda = 0.01$. Notice that the ACPR threshold is imposed by the LTE/5G standard specification equal to $\mathcal{M} = -45$dBc.

A. *Adaptive search for the pruned structure*

To verify the effectiveness of the proposed method, Fig. 3 shows the comparison of NMSE as a function of the number of coefficients. The DOMP only method is represented in green, the DOMP with ILA based on LS algorithm (DOMP+ILA (LS)) in blue, the DOMP with DLA based on classical Gradient (DOMP+DLA (Gradient)) in red, and the proposed method in orange.

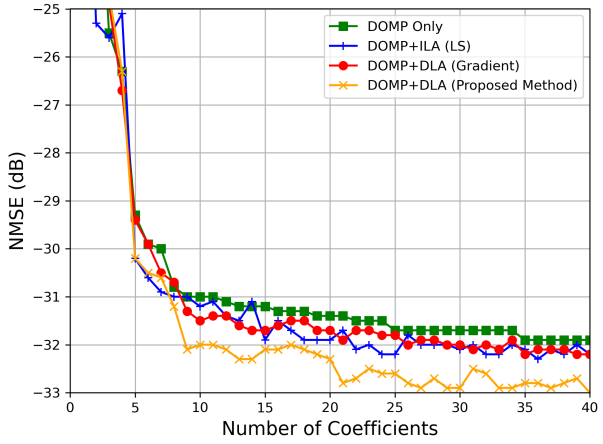

Fig. 3: Comparison of NMSE decrease versus the number of coefficients for DOMP Algorithm (green) DOMP only (blue) ILA based on LS algorithm (red) DLA based on Gradient (orange) proposed method.

As expected, the NMSE decreases as the number of coefficients increases for all methods. The DOMP only is used to obtain the pruned structure and also serves as a reference for initializing the other methods, hence its limited level of performance. The results show that the ILA and DLA methods have similar performance. However, from the 8^{th} coefficient, the proposed method outperforms both. Using 27 coeficients or more in the model, the NMSE reaches -32.9 dB, which in practice translates into an ACPR close to -45dBc.

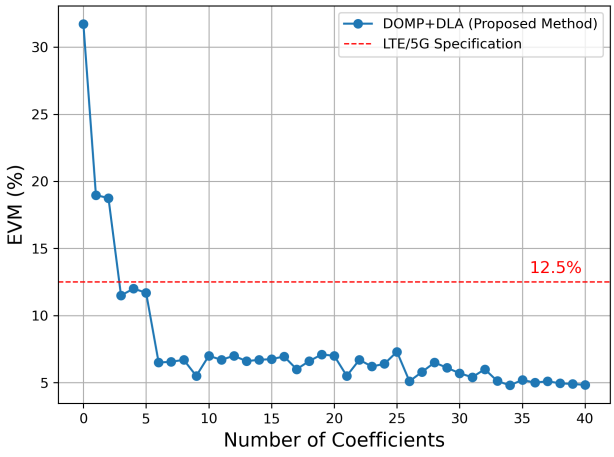

Fig. 4: Measured real-time EVM as function of number of coefficients for the proposed method

Fig. 4 shows the evolution of the EVM for the proposed method. In mobile communications, the Error Vector Magnitude (EVM) represents the percentage performance of a communication system under impairments. It measures the deviation in magnitude and phase by comparing the

received symbols with the transmitted ones. In LTE/5G, the specifications set a minimum EVM requirement of 12.5%. Similar to the NMSE results, the EVM decreases as the number of coefficients increases. For a pruned structure with approximately six coefficients, a significant improvement is observed, reducing from 30% to 8%. This reflects the contribution of active terms to the accuracy of linearization.

B. Linearization results

In this section, we present the linearization results in terms of NMSE and ACPR by comparing methods with a pruned structure of 30 coefficients and a full structure of 72 coefficients. It is worth noting that the pruned structure with 30 coefficients represents a good trade-off between complexity and performance in terms of EVM and ACPR. In Fig. 5, we show the NMSE convergence during the recursive process for several structures and algorithms. The Full DLA (Gradient) is shown in green, the Full ILA (LS) in black. These two methods correspond to the full GMP structure with 72 coefficients. Additionally, the DOMP+ILA (LS) is represented in blue, the DOMP+DLA (Gradient) in red, and the proposed method in orange. These three methods are evaluated with 30 coefficients, which was identified as an optimal pruned structure in the previous section.

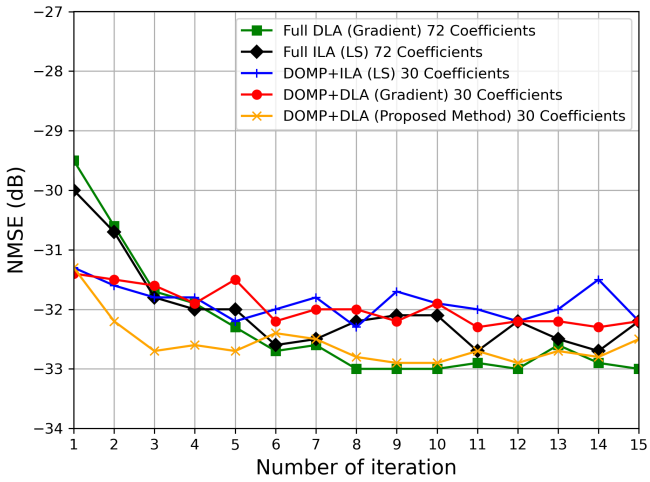

Fig. 5: Comparison of NMSE versus the number of iterations during the recursive process for full (green) DLA (black) ILA and pruned DOMP algorithm based on (blue) ILA/LS (red) DLA/Gradient (orange) proposed method.

As we can see, the NMSE of linearization (error between the PA input and output) decreases as the number of iterations increases. The lowest NMSE of -33 dB is achieved with the Full DLA (Gradient), which outperforms the other methods by up to 1 dB. However, the proposed method converges faster than the other methods, which is the advantage of the L-M algorithm. The remaining methods exhibit relatively similar performance. These results confirm that Levenberg-Marquardt algorithm enhances convergence and achieves performance close to that of the full-structure models while using a reduced number of coefficients.

Table II shows the ACPR comparison for different bandwidths (5, 10 and 20 MHz) with and without DPD. The ACPR quantifies, in dBc (dB relative to the carrier), the spectral regrowth in the upper and lower sidebands and indicates the level of linearity. Note that the LTE/5G standard imposes a maximum ACPR of -45 dBc.

BW	Condition	ACPR Lower (dBc)	ACPR Upper (dBc)
5MHz	without	-35.82	-35.89
	with DPD	-48.67	-48.19
10MHz	without	-34.83	-33.78
	with DPD	-47,52	-46,23
20MHz	without	-36.06	-34.44
	with DPD	-45,00	-44,83

TABLE II: ACPR comparison for different bandwidths

We can see that without DPD, the PA has a very low ACPR value because it is designed using the Doherty architecture to improve power and efficiency performance rather than linearity. The pruned DPD significantly improves the linearity of the global system with 10 to 13 dB of improvement.

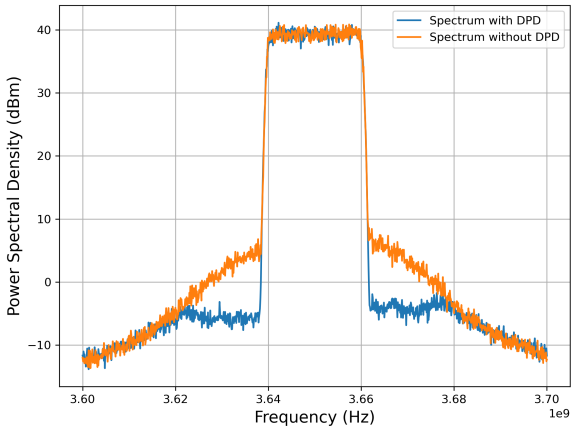

Fig. 6: Power spectral density with and without DPD

To illustrate the linearization performances, the measured spectrum for 20 MHz bandwidth with and without DPD are shown in Fig. 6. We can observe the effectiveness of the pruned structure in term of spectral regrowth reduction. We can notice an improvement of about 10 dB in the lower and upper first sidebands.

The original and linearized AM/AM and AM/PM characteristics are presented in Fig. 7. With DPD, the gain nonlinearity is well corrected in the nonlinear region. Similarly, a lower dispersion of the phase characteristics is observed.

IV. Conclusion

In this paper, an adaptive pruning method for the GMP model is proposed, improving the search for the optimal DPD structure using the DLA algorithm, which includes the

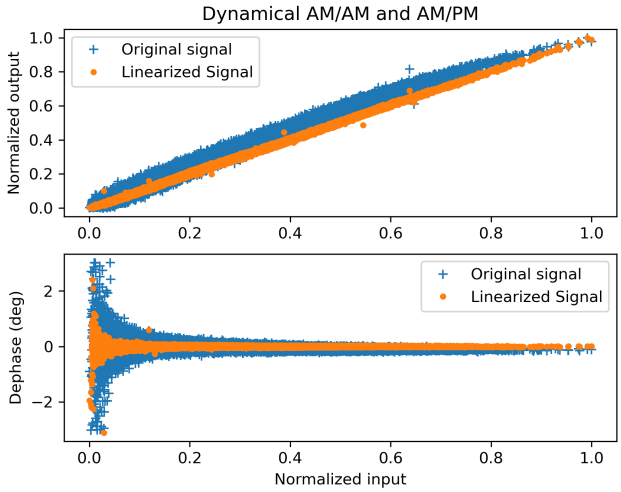

Fig. 7: Dynamical AM/AM and AM/PM characteristics with and without DPD

DOMP method and the L-M algorithm. The main principle is to extract the efficient terms based on the complexity of the implementation (number of coefficients) and standard requirements (ACPR and EVM thresholds). The proposed method differs from the classical DLA in several ways. It ensures the convergence of the calculation process through appropriate initialization settings provided by the DOMP method. Additionally, it updates the coefficients using the L-M expression, which improves robustness and convergence to the optimal values. As a result, this method reduces complexity and enhances stability. Furthermore, it can dynamically add or remove basis GMP terms in response to environmental changes in the PA, such as temperature drift, supply bias, or component aging.

This method has been tested using a Doherty power amplifier designed for high power and efficiency. For 20 MHz bandwidth, without DPD, an ACPR of -35 dBc is measured, which falls short of the -45 dBc required by the LTE-A and 5G standards. With the proposed algorithm, the iterative method searches for a lower-complexity model that includes only the most active terms. For a structure with 30 coefficients, measurements show an ACPR below -45 dBc across several frequency bands. With this signal, the NMSE reaches -33 dB, with an EVM of 6%.

Acknowledgment

The research reported in this publication is part of the RapidX project, supported by the RapidSpace Society. The authors are grateful to its members for providing the ORS box and for their valuable technical support.

References

[1] D. Morgan, Z. Ma, J. Kim, M. Zierdt, and J. Pastalan, "A generalized memory polynomial model for digital predistortion of rf power amplifiers," *IEEE Transactions on Signal Processing*, vol. 54, no. 10, pp. 3852–3860, 2006.

[2] C. Kantana, *System Approach for Optimizing a Low-Complexity Digital Predistortion Model for RF Power Amplifier Linearization*. Theses, Universite Paris-Est, Dec. 2021.

[3] C. Quindroit, P. Rochas, N. Monsauret, and A. Courty, "Study of high frequency nonlinear memory effect on doherty power amplifiers linearization performances for 5g applications," in *2023 IEEE Topical Conference on RF/Microwave Power Amplifiers for Radio and Wireless Applications*, pp. 49–52, 2023.

[4] J. Pedro and S. Maas, "A comparative overview of microwave and wireless power-amplifier behavioral modeling approaches," *IEEE Transactions on Microwave Theory and Techniques*, vol. 53, no. 4, pp. 1150–1163, 2005.

[5] H. E. Hamoud, T. Reveyrand, S. Mons, and E. Ngoya, "A comparative overview of digital predistortion behavioral modeling for multi-standards applications," in *2018 International Workshop on Integrated Nonlinear Microwave and Millimetre-wave Circuits (INMMIC)*, pp. 1–3, 2018.

[6] J. Kim and K. Konstantinou, "Konstantinou, k.: Digital predistortion of wideband signals based on power amplifier model with memory. iee electronics letters 37, 1417-1418," *Electronics Letters*, vol. 37, pp. 1417 – 1418, 12 2001.

[7] L. Ding, G. Zhou, D. Morgan, Z. Ma, J. Kenney, J. Kim, and C. Giardina, "A robust digital baseband predistorter constructed using memory polynomials," *IEEE Transactions on Communications*, vol. 52, no. 1, pp. 159–165, 2004.

[8] M. Abi Hussein, V. A. Bohara, and O. Venard, "On the system level convergence of ila and dla for digital predistortion," in *2012 International Symposium on Wireless Communication Systems (ISWCS)*, pp. 870–874, 2012.

[9] C. Yu, K. Tang, and Y. Liu, "Adaptive basis direct learning method for predistortion of rf power amplifier," *IEEE Microwave and Wireless Components Letters*, vol. 30, no. 1, pp. 98–101, 2020.

[10] A. Zhu and T. Brazil, "Behavioral modeling of rf power amplifiers based on pruned volterra series," *IEEE Microwave and Wireless Components Letters*, vol. 14, no. 12, pp. 563–565, 2004.

[11] M. Alizadeh, P. Händel, and D. Rönnow, "Behavioral modeling and digital pre-distortion techniques for rf pas in a 3 × 3 mimo system," *International Journal of Microwave and Wireless Technologies*, vol. 11, no. 10, p. 989–999, 2019.

[12] S. Wang, *Study on complexity reduction of digital predistortion for power amplifier linearization*. Theses, Université Paris-Est, Jan. 2018.

[13] S. Wang, M. Abi Hussein, O. Venard, and G. Baudoin, "Optimal sizing of two-stage cascaded sparse memory polynomial model for high power amplifiers linearization," *IEEE Transactions on Microwave Theory and Techniques*, vol. 66, no. 9, pp. 3958–3965, 2018.

[14] O. Lee, K. H. An, C.-H. Lee, and J. Laskar, "A parallel-segmented monolithic step-up transformer," *IEEE Microwave and Wireless Components Letters*, vol. 21, no. 9, pp. 468–470, 2011.

[15] Y.-J. Liu, J. Zhou, W. Chen, and B.-H. Zhou, "A robust augmented complexity-reduced generalized memory polynomial for wideband rf power amplifiers," *IEEE Transactions on Industrial Electronics*, vol. 61, no. 5, pp. 2389–2401, 2014.

[16] F. Mkadem, A. Islam, and S. Boumaiza, "Multi-band complexity-reduced generalized-memory-polynomial power-amplifier digital predistortion," *IEEE Transactions on Microwave Theory and Techniques*, vol. 64, no. 6, pp. 1763–1774, 2016.

[17] J. A. Becerra, M. J. Madero-Ayora, J. Reina-Tosina, C. Crespo-Cadenas, J. García-Frías, and G. Arce, "A doubly orthogonal matching pursuit algorithm for sparse predistortion of power amplifiers," *IEEE Microwave and Wireless Components Letters*, vol. 28, no. 8, pp. 726–728, 2018.

[18] D. W. Marquardt, "An algorithm for least-squares estimation of nonlinear parameters," *Journal of the Society for Industrial and Applied Mathematics*, vol. 11, no. 2, pp. 431–441, 1963.

[19] H. Wang, F. Liu, and W. Tao, "Robust and fast iterative algorithm based on levenberg-marquardt and spectral extrapolation for wideband digital predistortion of rf power amplifiers," in *2015 IEEE International Wireless Symposium (IWS 2015)*, pp. 1–4, 2015.

[20] L. Ljung, *System Identification: Theory for User*. Prentice Hall, USA, 1987.